Biased AC Electrospinning of Aligned Polymer Nanofibers

Soumayajit Sarkar, Seetharama Deevi, Gary Tepper*

A new method is reported for minimizing the inherent fiber instability in the electrospinning process. The method, dubbed "biased AC electrospinning", employs a combination of DC and AC potentials and results in highly-aligned mats of polymer or composite polymer fibers. The relationship between specific processing variables such as the AC frequency and the magnitude of the DC offset was investigated and related to the resulting fiber stability and uniformity. For optimum fiber stability, the AC frequency must fall within a relatively narrow range. The upper and lower frequency limits were measured for a small group of polymers and polymer composites and were qualitatively related to solution properties and processing variables. Potential applications of well-ordered nanofiber materials include tissue engineering, filtration, drug delivery, and microelectronics.

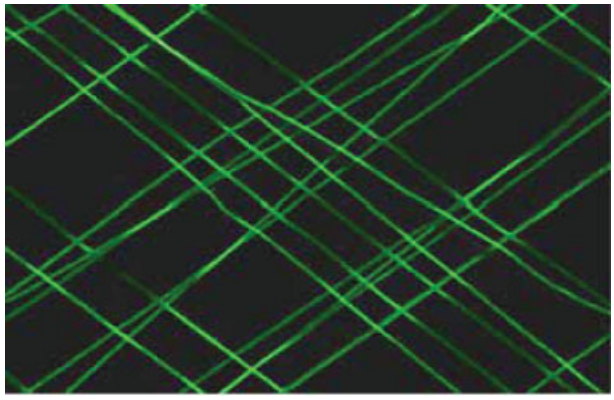

Introduction

Electrospinning is being widely investigated as a simple and robust technique for the production of submicron polymer fibers for applications ranging from filtration to drug delivery and tissue engineering.[1–10] Because electrostatic, rather than mechanical, forces are used to draw polymer fibers from a solution, the mean fiber diameter can be quite small and is often below 100 nm.[11,12] However, electrospun fibers, during formation, are electrically charged and inherently unstable and the materials or mats produced from the fibers usually exhibit a random, non-woven microstructure.[13–15] In many emerging applications, the ability to precisely control the polymer nanofiber alignment and orientation would provide a significant performance advantage.

Various techniques have been investigated in an attempt to produce well-aligned electrospun fibers but with only a limited success.[16–23] Examples include increasing the rotational speed of the collecting drum, introducing a potential across a gap or series of gaps in the collecting electrode, introducing an external lens element or a viscous liquid environment, or rapidly oscillating a grounded frame within the liquid jet. All of these methods rely on minimizing the fiber instability by applying external forces on the fibers during production. In this manuscript, we report on a new method for minimizing

S. Sarkar, G. Tepper
Department of Mechanical Engineering, Virginia Commonwealth University, Richmond, VA, USA
E-mail: gctepper@vcu.edu
S. Deevi
Philip Morris USA, Richmond, VA, USA

Macromol. Rapid Commun. **2007**, *28*, 1034–1039

DOI: 10.1002/marc.200700053

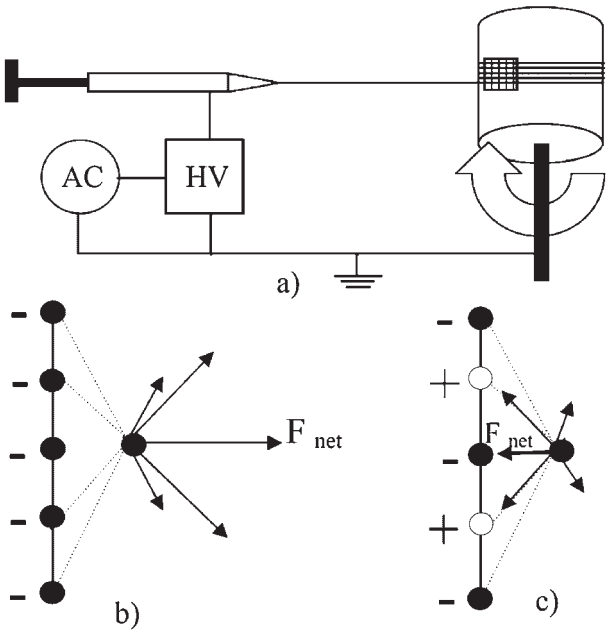

Figure 1. (a) Schematic diagram of the electrospinning apparatus. Force balance on a displaced segment of an electrically charged fiber in (b) DC electrospinning and (c) AC electrospinning.

the inherent instability of the fiber itself, thereby, eliminating the need to modify the apparatus or apply any additional external forces.

Previously, we demonstrated the possibility of increasing the alignment in electrospun fibers through the use of an alternating (AC) instead of the conventional (DC) voltage for fiber generation.[24] The applied AC voltage introduces alternating positively and negatively charged regions in the fiber, resulting in a decrease in electrostatic repulsion and an increase in fiber stability. Figure 1(a) is a schematic diagram illustrating the primary components of the electrospinning apparatus and Figure 1(b) and 1(c) contrast the force balance on a charged fiber of single polarity (b) versus a charged fiber produced using an AC potential and containing alternating positively and negatively charged regions (c). For a fiber with a single charge polarity, it is well established that small fiber deformations are amplified through repulsive Coulombic forces leading to the widely observed fiber instability.[13–15] For a fiber with alternating regions of positive and negative charge, on the other hand, both attractive and repulsive Coulombic forces are involved and a corresponding decrease in the overall instability is observed.[24] However, when a pure AC potential is used, the net charge on the fiber is very small (approaching 0) resulting in a correspondingly small attractive force between the fiber and the collecting electrode, making fiber collection somewhat challenging.

Here, we report new results where the attractive or drawing force on the fiber is increased; while at the same time the fiber instability is minimized by applying a DC biased AC potential instead of either a pure AC or DC potential. Fiber mats were collected for several polymers and polymer composites, the average fiber diameter and the degree of alignment were determined as a function of the DC bias and the AC amplitude and frequency. We found that a very high degree of fiber uniformity and alignment could be achieved for each polymer/solvent system investigated in this study as long as the following two general process requirements were followed:

(i) The magnitude of the DC bias must be less than half the total amplitude of the AC potential.
(ii) The AC frequency should be between 500 and 1 000 Hz for optimum fiber stability.

Experimental Part

Poly(ethylene oxide) (PEO), polyisobutylene (PIB), and polystyrene (PS) (all from Aldrich Chemicals) were used as prototypical polymers in this study. In addition, PEO composite fibers consisting of PEO blended with either single-walled carbon nanotubes (SWCNT), gold nanoparticles, or FeAl nanoparticles were studied. The single-walled carbon nanotubes (SWCNT) were obtained from Carbon Solutions, the gold nanoparticles were obtained from Aldrich Chemicals, and the FeAl nanoparticles were produced in the VCU chemistry department using a laser ablation process.[25,26] Toluene and ethanol were used as the electrospinning solvents and were obtained from Aldrich Chemicals and were of HPLC grade. All the polymers were used without additional purification. The range of electrospinning experimental conditions are summarized in Table 1.

A waveform generator was used to provide the AC signal in the form of a square wave with adjustable amplitude, duty cycle, and frequency. A high voltage amplifier having a maximum output of $-10\,000$–$+10\,000$ V_{ac} and frequency range of DC to 30 kHz was used to amplify the output of the waveform generator. The high voltage amplifier has a biasing feature, which was used to bias the AC voltage to a desired DC value. The liquid flow-rate to the electrospinning needle was controlled using a syringe pump. The electrospinning source consisted of a syringe with a 27-gauge tip. The AC potential, frequency, biasing value, flow rate, and distance between the needle and the target were adjusted to obtain a stable fiber and the resulting fibers' mats were characterized by a JOEL scanning electron microscope (SEM), LEO SEM, and an optical microscope (Olympus BX60).

Figure 2(a) and 2(b) show a set of SEM images of typical PEO fiber mats collected under pure AC and pure DC potentials. While the AC potential significantly increased the degree of fiber alignment in comparison to the DC potential, the AC-spun fibers exhibit a relatively large variation in diameter attributed to the very low overall drawing force on the fiber.

Figure 2(c–f) show a set of scanning electron microscope images for mats of pure PEO and three PEO composite fibers produced

Table 1. Experimental conditions for obtaining aligned fibers using an AC voltage with a biased DC component.

Polymer/polymer nanocomposite	Polymer concentration	AC voltage	DC biased value	Frequency	Flowrate	Needle to target distance
	wt.-%	kV_{p-p}	kV	Hz	$\mu L \cdot min^{-1}$	cm
PEO	8	9.5	4	400–1 000	0.8	7.0
PEO + Single-walled carbon nanotubes	8	9.3	4.1	500–1 000	0.8	7.0
PEO + Au nanoparticles	10	9.3	4.2	500–1 000	1.0	7.0
PEO + FeAl nanoparticles	6	9.5	3.8	550–1 000	0.7	7.0
PS	20	11	5.2	300–700	0.6	7.0
PIB	15	12	5.5	400–700	1.2	7.0

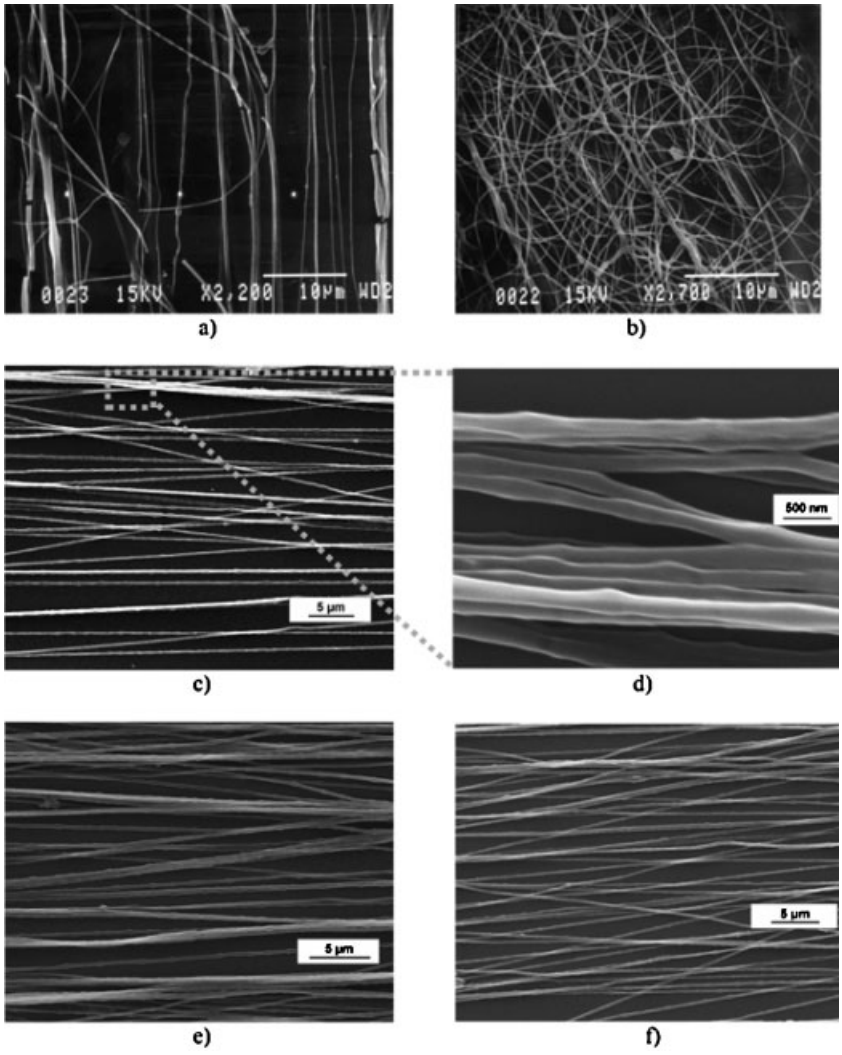

Figure 2. (a) AC electrospun PEO at 5 000 V_{p-p} and 60 Hz. (b) DC electrospun PEO at 6 000 V. (c) PEO with SWNT at a biased voltage of 4 100 V and AC voltage of 9 300 V_{p-p} and 600 Hz. (d) Higher magnification image of a section from image c. (e) PEO nanofibers at a bias voltage of 4 000 V and AC voltage of 9 500 V_{p-p} and 600 Hz. (f) PEO with Au nanoparticles at a bias voltage of 4 200 V and AC voltage of 9 300 V_{p-p} and 600 Hz.

Macromol. Rapid Commun. **2007**, *28*, 1034–1039

Macromolecular Journals

DOI: 10.1002/marc.200700053

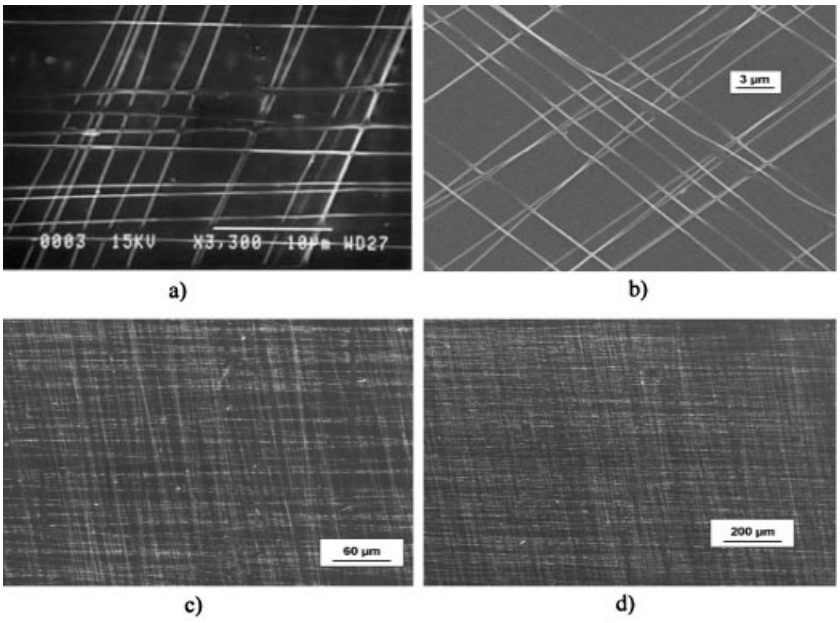

Figure 3. (a) Wire mesh of PEO with single-walled carbon nanotubes. (b) Wire mesh of polystyrene. (c) and (d) Reduced magnification image of PEO/SWCNT mesh.

using the biased AC electrospinning method and using the processing conditions summarized in Table 1. A solution of 8 wt.-% PEO in DI water was prepared. The SWCNTs were added to a water solution with sodium dodecyl benzene sulfonate, which acts as a surfactant. The SWCNT solution was then mixed in a homogenizer for 5 h and the 8 wt.-% PEO solution was added to the resulting solution. The addition of the PEO solution to the agitated solution of SWCNT resulted in a relatively homogeneous dispersion. Thus, the final solution has a composition of 8 wt.-% PEO solution in water with 2.5 wt.-% SWCNT. Similarly, a solution of 6 wt.-% PEO in DI water was prepared and 2.4 wt.-% of FeAl nanoparticles were added after 5 h in a homogenizer. The resultant solution consisted of a 6 wt.-% PEO solution with 2.4 wt.-% FeAl nanoparticles by weight with respect to the polymer. Also, a 10 wt.-% solution of PEO was prepared in DI water. 2 wt.-% Au nanoparticles with respect to the weight of the polymer were added to DI water along with 0.4 wt.-% sodium dodecyl benzene sulfonate and homogenized for 5 h. The polymer solution was slowly added to this agitated solution. The resultant mixture is a 10 wt.-% PEO solution with 2 wt.-% Au nanoparticles by weight with respect to the polymer.

Results

The fibers in the mats shown in Figure 2(c–f) were found to be highly aligned, very uniform, and typically between 300 and 500 nm in diameter. The magnitude of the DC bias was chosen such that the bottom edge of the negative half-cycle of the AC voltage just crosses zero and becomes negative, thereby introducing a negative charge on the fiber during every other half cycle. The optimum frequency range was found to generally fall between 500 Hz and 1 kHz. However, the specific frequency range for stable fiber formation was slightly different for each polymer/solvent system. Highly aligned mats of PIB and PS polymer nanofibers were also produced using the biased AC electrospinning method. Images of these mats are omitted for brevity because they appear identical to the PEO images shown in Figure 2(c–f).

Figure 3 is a scanning electron microscope image of some more advanced PEO and PS nanofiber structures produced using the biased AC technique. A set of aligned fibers was deposited and then the collecting target was rotated by approximately 90° and a second set of aligned fibers was deposited onto the same collector, thereby producing a mesh pattern. The ability to precisely control the deposition of polymer nanofibers is useful for many applications including microelectronics, filters, and sensor devices.

Figure 4 is a plot of the stable frequency range for each polymer or polymer composite. The minimum and maximum stable frequencies are defined here for each polymer/solvent system as the frequency where the first visible onset of instability was observed. Instability onset was determined by visually monitoring the fibers as they are drawn from the needle to the collector and documenting the frequency when mechanical oscillations first become visible. A high-speed digital camera with a microscopic lens was used to monitor the stability of the small diameter fibers. The minimum and maximum stable frequencies varied for each polymer solution. However, the maximum frequency for the PEO and PEO composites was surprisingly consistent and was about 1 000 Hz, whereas

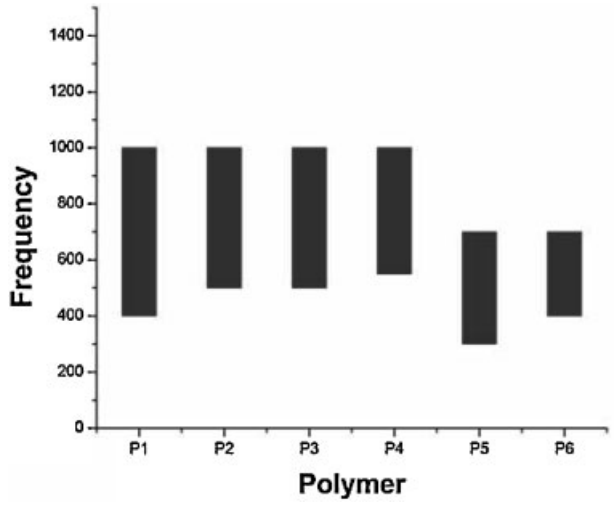

Figure 4. Stable frequency range for each of the six systems studied in this investigation. P1 = PEO, P2 = PEO with SWCNT, P3 = PEO with Au, P4 = PEO with FeAl, P5 = PS, P6 = PIB.

the maximum frequency for the PS and PIB polymer solutions was lower and around 700 Hz.

Discussion

We believe that the minimum frequency limit is related to the fiber production (draw) rate. That is, the AC frequency must be sufficiently high such that multiple positively and negatively charged regions are produced on the fiber before it traverses the distance between the source (needle) and collecting electrode. For example, for a typical flow rate of 1 $\mu L \cdot min^{-1}$ and assuming that the diameter of the jet of liquid emerging from the tip of the Taylor cone is approximately 10 μm, the fiber production rate is of the order of 20 $cm \cdot s^{-1}$. Therefore, it takes about 0.35 s for the fiber to traverse the 7 cm distance between the needle and the collector. An AC frequency of 500 Hz, would, therefore, produce about 175 positively charged regions and an equal number of negatively charged regions, each about 0.2 mm in length. It is interesting to note that the PS solution had the lowest flow rate (0.6 $\mu L \cdot min^{-1}$) and also the lowest stable AC frequency (300 Hz), which qualitatively agrees with this explanation of the relationship between fiber production rate and minimum frequency.

The high frequency limit, on the other hand, is determined by the ion mobility in each solution. That is, if the frequency is too high, the solution will be unable to reverse the charge polarity within a single cycle. We are currently developing a model incorporating the charge mobility information to predict the upper frequency limit as a function of solvent properties and this will be reported in a future publication. In addition, this model will be used to estimate the degree of attraction and self-neutralization of neighboring oppositely charged regions of a fiber.

The rotational speed of the collecting drum did not appear to influence the stability of the electrospun fibers, but could significantly impact the morphology of the collected fiber mat. For example, stable fibers could be deposited even onto a non-rotating substrate but would simply accumulate at one location. In contrast, unstable fibers could not be forced into an aligned array even under the highest rotational speeds of the collecting substrate used in this investigation.

Conclusion

The fiber instability in the polymer electrospinning process was eliminated through the use of a biased AC potential. Well-oriented arrays of submicron polymer and polymer composite fibers were produced and characterized as a function of processing conditions. Aligned fiber arrays have many potential applications in areas such as filtration, drug delivery, and tissue engineering.

Acknowledgements: This work was supported in part by a research contract from *Philip Morris* USA. The FeAl nanoparticles were provided by *Samy El-Shall* in the VCU Department of Chemistry.

Received: January 23, 2007; Revised: February 15, 2007; Accepted: March 1, 2007; DOI: 10.1002/marc.200700053

Keywords: composites; electrospinning; nanofibers; nanoparticles; polymers

[1] X. Fang, D. H. Reneker, *J. Macromol. Sci., Part B: Phys.* **1997**, *B36*, 169.
[2] J. Doshi, D. H. Reneker, *J. Electrostat.* **1995**, *35*, 151.
[3] A. G. MacDiarmid, W. E. Jones, I. D. Norris, J. Gao, A. T. Johnson, N. J. Pinto, J. Hone, B. Han, F. K. Ko, H. Okuzaki, M. Llaguno, *Synth. Met.* **2001**, *119*, 27.
[4] M. Wang, H. Singh, T. A. Hatton, G. C. Rutledge, *Polymer* **2004**, *45*, 5505.
[5] E. Kenawy, J. M. Layman, J. R. Watkins, G. L. Bowlin, J. A. Matthews, D. G. Simpson, G. E. Wnek, *Biomaterials* **2003**, *24*, 907.
[6] C.-W. Kim, M. W. Frey, M. Marquez, Y. L. Joo, *J. Polym. Sci., Part B: Polym. Phys.* **2005**, *43*, 1673.
[7] C. He, Z. Huang, X. Han, L. Liu, H. Zhang, L. Chen, *J. Macromol. Sci., Part B: Phys.* **2006**, *45*, 515.
[8] H. Jin, S. V. Fridrikh, G. C. Rutledge, D. L. Kaplan, *Biomacromolecules* **2002**, *3*, 1233.
[9] C. Y. Xu, R. Inai, M. Kotaki, S. Ramakrishna, *Biomaterials* **2004**, *25*, 877.
[10] F. Yang, R. Murugan, S. Ramakrishna, X. Wang, Y. X. Ma, S. Wang, *Biomaterials* **2004**, *25*, 1891.

DOI: 10.1002/marc.200700053

[11] R. Sen, B. Zhao, D. Perea, M. E. Itkis, H. Hu, J. Love, E. Bekyarova, R. C. Haddon, *Nano Lett.* **2004**, *4*, 459.
[12] N. Bhattarai, D. Edmondson, O. Veiseh, F. A. Matsen, M. Zhang, *Biomaterials* **2005**, *26*, 6176.
[13] Y. M. Shin, M. M. Hohman, M. P. Brenner, G. C. Rutledge, *Polymer* **2001**, *42*, 09955.
[14] A. L. Yarin, S. Koombhongse, D. H. Reneker, *J. Appl. Phys.* **2001**, *89*, 3018.
[15] D. H. Reneker, A. L. Yarin, H. Fong, S. Koombhongse, *J. Appl. Phys.* **2000**, *87*, 4531.
[16] D. Sun, C. Chang, S. Li, L. Lin, *Nano Lett.* **2006**, *6*, 839.
[17] A. Babel, D. Li, Y. Xia, S. A. Jenekhe, *Macromolecules* **2005**, *38*, 4705.
[18] D. Li, M. Ouyang, J. McCann, Y. Xia, *Nano Lett.* **2005**, *5*, 913.
[19] D. Li, Y. Wang, Y. Xia, *Adv. Mater.* **2004**, *16*, 361.
[20] D. Li, Y. Wang, Y. Xia, *Nano Lett.* **2003**, *3*, 1167.
[21] P. Katta, M. Alessandro, R. D. Ramsier, G. G. Chase, *Nano Lett.* **2004**, *4*, 2215.
[22] E. Smit, U. Buttner, R. D. Sanderson, *Polymer* **2005**, *46*, 2419.
[23] X. Mo, H. Weber, *Macromol. Symp.* **2004**, *217*, 413.
[24] R. Kessick, J. Fenn, G. Tepper, *Polymer* **2004**, *45*, 2981.
[25] Y. B. Pithawalla, S. C. Deevi, M. S. El-Shall, *Mat. Sci. Eng., A: Struct. Mat. : Properties, Microstruct. Processing* **2002**, *A329*, 92.
[26] G. Glaspell, V. Abdelsayed, K. M. Saoud, M. S. El-Shall, *Pure Appl. Chem.* **2006**, *78*, 1667.